EBW simulation for MAST and NSTX experiments

J. Preinhaelter[1)], G. Taylor[2)], V. Shevchenko[3)], J. Urban[1)], M. Valovic[3)], P. Pavlo[1)], L. Vahala[4)], G. Vahala[5)]

1) EURATOM/IPP.CR Association, Institute of Plasma Physics, 182 21 Prague, Czech Republic
2) Princeton Plasma Physics Laboratory, Princeton, New Jersey 08543, USA
3) EURATOM/UKAEA Fusion Association, Culham Science Centre, Abingdon, OX14 3DB, UK
4) Old Dominion University, Norfolk, VA 23529, USA
5) College of William & Mary, Williamsburg, VA 23185, USA

Abstract. The interpretation of EBW emission from spherical tokamaks is nontrivial. We report on a 3D simulation model of this process that incorporates Gaussian beams for the antenna, a full wave solution of EBW-X and EBW-X-O conversions using adaptive finite elements, and EBW ray tracing to determine the radiative temperature. This model is then used to interpret the experimental results from MAST and NSTX. EBW for ELM free H-modes in MAST suggests that the magnetic equilibrium determined by the EFIT code does not adequately represent the B-field within the transport barrier [1]. Using the EBW signal for the reconstruction of the radial profile of the magnetic field, we determine a new equilibrium and see that the EBW simulation now yields better agreement with experimental results. EBW simulations yield excellent results for the time development of the plasma temperature as measured by the EBW radiometer on NSTX [2].

Keywords: Spherical tokamaks. Electron Bernstein waves.
PACS: 52.55.Fa, 52.35.Hr

Introduction

The characteristic low magnetic field and high plasma density of a spherical tokamak do not permit the typical radiation of O and X modes from the first five electron cyclotron harmonics. Thus only electron Bernstein waves (EBW), (modes not subject to a density limit), which mode convert into electromagnetic waves in the upper hybrid resonance region, can be responsible for the measured radiation [3]. The 3D plasma and antenna model was described in [1, 4, 5].

Magnetic Field Reconstruction from EBW Signal in MAST

We found good agreement between the simulation of EBW emission and the detected signals for L-modes and ELMy H-modes. On the other hand the emission from ELM free H-modes in MAST suggests that the magnetic field in the transport barrier as determined by EFIT is too low. Typically the detected signal in the 16-60GHz band has five peaks, each corresponding to the emission from subsequent electron cyclotron harmonics (see Fig. 1). The gaps between the peaks correspond to the frequencies at which the upper hybrid frequency coincides with some of the electron cyclotron harmonics. From the position of the gaps in the spectrum of the detected signal we can determine the magnitude of the magnetic field. The corresponding R position occurs

CP787, *Radio Frequency Power in Plasmas:16th Topical Conference on Radio Frequency Power in Plasmas*
edited by Stephen J. Wukitch and Paul T. Bonoli

where the upper hybrid frequency coincides with the frequency of the electron cyclotron harmonics (we investigate the shot where the detected signal originates in the equatorial plane). The profiles of the EFIT magnetic field and the reconstructed profile from EBW signal are given in Fig. 2. We assume that only the poloidal magnetic field is influenced at the transport barrier. The magnetic configuration in the rest of the plasma is assumed to be that determined by EFIT.

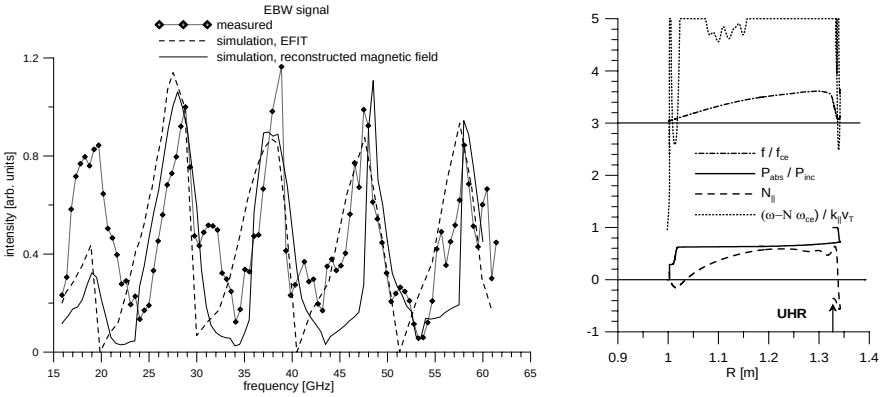

FIGURE 1. Comparison of the detected ECE signal and two simulations (EFIT magnetic equilibrium-blue line, and the equilibrium with a bump in the magnetic field profile at the transport barrier). #8694, t=280ms, the time corresponds to the final stage of the prolonged ELM free period of the H-mode shot. (**left**). Radial dependence of the wave and the plasma parameters along the EBW ray (**right**).

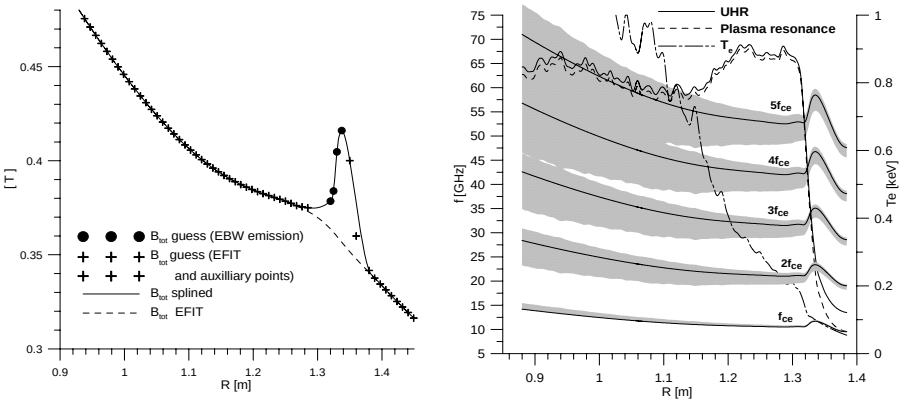

FIGURE 2: Comparison of the EFIT profile of the magnetic field and the field reconstructed from the EBW signal for #8694 (**left**). Radial profiles of the characteristic resonances in the equatorial plane (**right**).

To gain some insight into the significance of the proposed bump on the magnetic field we consider the radial profiles of the characteristic resonances (Fig. 2). The broadening of nf_{ce} is given by the factor $1/(1\pm 3N_{\|}(v_T/c))$. Rays with frequency

below nf_{ce} are usually emitted with $N_{||}=1$, while $N_{||}$ is oscillating for rays with frequency above nf_{ce}. Thus we consider an initial value of $N_{||}=0.36$. In the shaded areas EBW is strongly damped and the detected wave is emitted from the edges of these areas. The broadening of the gaps in the emitted spectrum (Fig. 1) is due to the bump on the magnetic field in the transport barrier. For the first two harmonics the magnetic field decreases in the transport barrier from the UHR region in the direction towards the plasma center. EBW with frequency slightly below nf_{ce} are then emitted from the rather cold plasma. On the other hand, EBW emitted slightly above the third and higher harmonics is strongly reabsorbed by the rarefied plasma in front of the UHR (see Fig. 1 right).

Here the ray is launched from the UHR region and starts to propagate out of the plasma. Its frequency is approaching the 3rd electron cyclotron harmonic (magnetic field increases in this direction due to the bump) and it is partially absorbed here. The ray is then reverted back to the dense plasma and is fully absorbed at the 3rd harmonics at the plasma center. Emission is the reverse process and the ray emitted from the plasma center where plasma temperature is 1keV is partly reabsorbed at the plasma boundary so finally T_{rad} = 0.7keV. Waves with slightly lower frequency (e.g., 37GHz) are fully absorbed at the plasma boundary with T_{rad} = 0.1keV only. The broadening of gaps due to the development of the bump in the magnetic field in the transport barrier can thus explain the observation of the missing EBW emission for some well-developed ELM free H-modes.

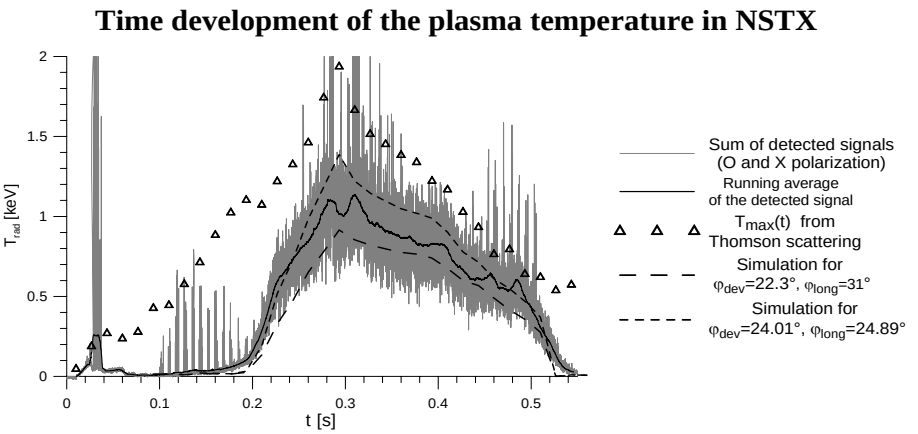

FIGURE 3: The time development of EBW signal (sum of O and X channels) detected by the NSTX antenna operating at 16.5GHz. #113544.

One of the most important results deduced from EBW emission measurements on NSTX is the time development of the radiation plasma temperature [2]. The obliquely viewing EBW radiometer on NSTX detects signals polarized parallel and perpendicular to the magnetic field at the EBW mode conversion layer. Since the outgoing O-mode at oblique incidence is approximately circularly polarized, the sum of these signals can be interpreted as a radiation temperature. We have performed

simulations of the time development of ECE in the interval $0.09s < t < 0.6s$. In Fig. 3, the time evolution of the sum of the EBW radiometer signals is plotted along with the maximum temperature detected by Thomson scattering (this independent measurement for $0.1s < t < 0.5s$ corresponds well to the temperature at $R = 1.007\ m$) and the theoretical simulation of EBW radiometer signals of Gaussian beams corresponding to actual antenna orientation (angles $\phi_{dev} = 23.3^{o}$, $\phi_{long} = 31^{o}$) as well as to orientations that are optimal for $EBW - X - O$ mode conversion (angles $\phi_{dev} = 24.01^{o}$, $\phi_{long} = 24.89^{o}$). The signal is proportional to the central temperature only for $t > 0.3s$ when the plasma current and the poloidal magnetic field reach their stationary values. For $t < 0.3s$, EBW is emitted from the 2nd electron cyclotron harmonic at the plasma periphery, where the plasma temperature is low. The simulation shows that the conversion efficiency for EBW-X-O is optimal and practically constant for $t \in (0.2s, 05s)$.

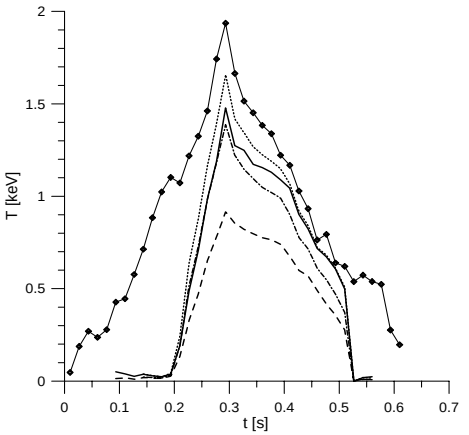

FIGURE 4: Time development of the central temperature (diamonds), a simulation for EBW effective temperature for optimum antenna angles (dotted), and for actual antenna angles (solid) as well as their reduced values (only these can be detected in the experiment) by the corresponding conversion efficiencies (dot-and-dash and dashed).

Simulations also clarify the relationship between the central temperature derived from the EBW signal and the temperature determined from Thomson scattering. We can state that the EBW temperature is always less than the actual temperature. In Fig 4 we depict the ideal effective temperature of EBW radiation for conversion efficiency equal 1. Even these values are smaller than T_{Thomson} because of reabsorption of EBW and the parasitic radiation from the second harmonic [2]. The intensity of EBW radiation is further reduced by losses due to imperfect conversion. This last effect is more pronounced if the antenna does not have optimum orientation.

Acknowledgments

Supported by U.S. Dept. of Energy, by UK Engineering and Physical Sciences Research Council, by EURATOM and by AS CR project #AV0Z-20430508.

References

1. J. Preinhaelter, V. Shevchenko, M. Valovic, et al., ECA **Vol. 28G**, P-4.184 (2004).
2. G. Taylor, P.C. Efthimion, B.P. LeBlanc, et al., Phys. Plasmas (2005) to be published
3. H.P. Laqua , et al., review, 15th RF Power in Plasma, Moran, 2003, edit. C. Forest, AIP **694**, 5.
4. J. Preinhaelter, V. Shevchenko, M. Valovic, et al., edit. C. Forest, AIP **694**, 388.
5. J. Preinhaelter, J. Urban, P. Pavlo, *et al.*, Review of Scientific. Instruments., Vol. 75, (2004), p 3804.